

Mono and Bifunctional Pathways of CO₂/CH₄ Reforming over Pt and Rh Based Catalysts

J. H. Bitter, K. Seshan, and J. A. Lercher¹

Faculty of Chemical Technology, Catalytic Processes and Materials, University of Twente, P.O. Box 217, 7500 AE, Enschede, The Netherlands

Received July 23, 1997; revised December 10, 1997; accepted December 10, 1997

Despite the high thermodynamic driving force to form coke under the reaction conditions applied Pt/ZrO₂ and Rh supported on γ -Al₂O₃ and ZrO₂ are active and stable catalysts for CO₂/CH₄ reforming. Using steady state, transient kinetic measurements and physico-chemical characterization techniques have shown that the catalyst activity is determined by the available Pt–ZrO₂ perimeter. Methane is decomposed on the metal to CH_x (average value of $x = 2$) and H₂. The main route to CO₂ reduction occurs via initial formation of carbonate close to the metal-support boundary. Carbon on the metal reduces that carbonate to formate by forming CO. The formate decomposes rapidly to CO and a surface hydroxyl group. Hydroxyl groups recombine and form water or react further with methane to CO and hydrogen (steam reforming). When the rate of methane decomposition and carbonate reduction are in balance, the catalytic activity remains stable. In contrast, the activity of Rh is mainly determined by the concentration of accessible surface atoms and a concerted metal catalyzed mechanism of methane decomposition and subsequent CO₂ reduction dominates. The support plays a minimal role in that chemistry. © 1998 Academic Press

INTRODUCTION

Carbon dioxide reforming of methane (CO₂ + CH₄ → 2CO + 2H₂) is an important route to produce pure CO or synthesis gas with a low H₂/CO ratio (1–4), e.g., to produce alcohols via the oxoalcohol synthesis (5), dimethyl ether, and acetic acid (6).

The major disadvantage of CO₂/CH₄ reforming is the high thermodynamic potential to form coke (2, 7–9). This coke rapidly deactivates the catalyst. Two commercial processes exist today which seem to have overcome this problem. One is the SPARG process using a Ni catalyst for which the coke formation is reduced by controlling the Ni ensemble size via adding sulfur compounds to the feed (7). The other is the CALCOR process operated at Caloric GmbH claiming that a special packing of the catalyst prevents carbon formation (5, 10). This is, however, not described in detail. Both processes have drawbacks affiliated with catalyst stability caused by rapid changes

in the feed (robustness of the system) or the presence of sulfur compounds in the products. Therefore, a strong incentive exists to re-examine the mechanistic aspects of dry reforming of methane in the quest to produce a stable catalyst with low tendency to form coke.

As early as 1928 Fischer and Tropsch showed that most group VIII metals display an appreciable activity for CO₂/CH₄ reforming (11). Much later, the problem has been revisited and various transition metals (Ni, Ru, Rh, Pt, Pd) have been tested (1, 8, 12–15). Despite a controversial debate about the most suitable metal, Rh was unanimously observed to be among the most stable and active of group VIII metals. Different supports were explored for the catalysts (2, 8, 15–18) and the most suitable support seemed to be Al₂O₃. Although Rh/ γ -Al₂O₃ is, thus, identified as a suitable catalyst for CO₂/CH₄ reforming, we have developed a Pt/ZrO₂ catalyst which is excellently suited for dry methane reforming being stable for 500 h time on-stream (19–21) and is clearly superior for industrial application (22).

In principle two mechanisms for CO₂/CH₄ reforming are discussed in the literature. Mark *et al.* (17, 23) and Erdöhelyi *et al.* (24) suggest an Eley Rideal type mechanism in which methane is adsorbed and decomposed on the metal (Rh) to H₂ and adsorbed carbon. The carbon on the catalyst reacts directly with CO₂ from the gas phase to CO.

In the alternative mechanism (2, 8, 12, 15, 25–28) methane is decomposed on the metal to yield a surface CH_x species and hydrogen. Upon sorption, carbon dioxide dissociates to CO and adsorbed oxygen. That oxygen reacts with the CH_x species to CO and hydrogen. While it is agreed that the CH_x species are formed on the metal, the nature of carbon dioxide activation is unclear. Qin *et al.* suggest that CO₂ dissociates on the metal to form M–CO and M–O (8). This is also supported by Bodrov *et al.* for CO₂/CH₄ reforming over a Ni foil (27). Bradford *et al.* (25), in contrast, suggest that adsorbed hydrogen reacts with CO₂ to form CO and an OH group (retained on the support). However, it is not clear whether CO₂ is activated on the support or if the metal is involved. The OH groups were thought to react at the metal-support interface with CH_x, resulting from

¹ E-mail: J.A.Lercher@utct.ct.utwente.nl

methane decomposition, to form CH_xO species which subsequently decompose to CO and H_2 .

In this context it is important to mention that Nakamura *et al.* (29) observed an increase in the activity for Rh/SiO₂ when γ -Al₂O₃, TiO₂, and MgO were added to the support. This was attributed to enhanced CO₂ activation on the support. Zhang *et al.* (30) attributed the remarkable stability of Ni/La₂O₃ compared to Ni/ γ -Al₂O₃ or Ni/CaO, also, to the fact that La₂O₃ activates CO₂ in the form of La₂O₂CO₃.

Earlier work from our group also showed that the support has a significant influence on the activity of the Pt catalyst (31). Unsupported Pt-black and Pt/SiO₂ showed only a very low activity, whereas Pt/ γ -Al₂O₃, Pt/TiO₂, and Pt/ZrO₂ were active catalysts (31). Also, the observation that the activity of Pt/ZrO₂ catalysts could be correlated to the length of the Pt-ZrO₂ perimeter indicated the significance of the support (31).

In this contribution we will address the involvement of the individual phases Pt and ZrO₂ in Pt/ZrO₂ and Rh in Rh/ γ -Al₂O₃ and Rh/ZrO₂ catalysts in the reaction mechanism and discuss their influence on the elementary steps.

EXPERIMENTAL

Catalyst preparation. The catalyst was prepared by the wet impregnation technique. For this purpose a solution of H₂PtCl₆ · 6H₂O in water (0.01 g Pt per ml) was used. The ZrO₂ (RC-100, Gimex, The Netherlands) was isostatically pressed into pellets at 4000 bars for 5 min. The pellets were crushed and sieved to give grains having diameters between 0.3 and 0.6 mm. The ZrO₂ grains were first calcined for 15 h at 1125 K (heating rate 3 K/min) in flowing air (30 ml/min (NTP)). The grains were impregnated with H₂PtCl₆ solution to yield a catalyst with 0.5 wt% Pt. The catalyst was dried at 365 K for 2 h in a rotating evaporator followed by drying over night at 395 K in static air. Subsequently, the impregnated grains were calcined at 925 K for 15 h (heating rate 3 K/min). The Pt content of the catalyst was determined by atomic absorption spectroscopy.

Unsupported Pt was prepared as described by Paal *et al.* (32). However, we used Pt-metal instead of H₂PtCl₆ as the starting material; 5 g of Pt-metal were dissolved in 100 ml aqua regia. To remove the excess of nitric acid, the solution was concentrated to a syrup. Subsequently, concentrated HCl was added and the solution was concentrated again. This procedure was repeated three times (33). The resulting orange syrup was dissolved in 50 ml of water and cooled to 273 K. 100 ml of hydrazine (in 400 ml of water) were slowly added, which resulted in the formation of a grey precipitate. After stirring overnight at room temperature the precipitate was filtered and washed thoroughly with water. The grey solid was dried at 393 K for several hours in air and subsequently reduced at 1025 K in 5% H₂/N₂. The

BET surface area of the resulting metal was 0.25 m²/g and its hydrogen chemisorption capacity (H/Pt) was 0.001.

Unsupported Rh sponge was used as obtained. Prior to testing, the metal was reduced *in situ* at 1025 K. The hydrogen chemisorption capacity of the metal after reduction was H/Rh = 0.0008.

XAS measurements. XAS measurements were performed at the Synchrotron Facility in Daresbury (beamline 9.2). The catalyst powder was pressed into a self-supporting wafer (110 mg). The catalysts were *ex situ* reduced at the desired temperature. Prior to the EXAFS experiments catalysts were rereduced *in situ* at 775 K. EXAFS measurements were carried out at liquid nitrogen temperature. To isolate the EXAFS from the X-ray absorption edge, a polynomial function characteristic of the background was subtracted. The oscillations were normalized by the mass areal loading of Pt. The oscillations were k²-weighted and Fourier transformed within the limits k = 3.5 to k = 18 to isolate the contributions of the different coordination shells.

IR spectroscopic measurement of CO₂ adsorption on Pt/ZrO₂. The catalyst powder was pressed into a self-supporting wafer. This wafer was analysed *in situ* during the reaction by means of transmission absorption IR spectroscopy using a Bruker IFS 88 FTIR spectrometer (resolution 4 cm⁻¹). The IR cell was constructed as a continuously stirred tank reactor (volume 1.5 cm³) equipped with 1/16-in. gas in- and outlet tubings and CaF₂ windows. The partial pressure of each of the reactants (CO₂ and CH₄) was 250 mbar, the difference to 1 bar being He and N₂.

Catalyst testing. Typically 300 mg of catalyst were loaded into a tubular quartz reactor (inner diameter 5 mm) which was placed in an oven. The catalyst grains were kept in place by quartz wool plugs. A thermocouple was placed on top of the catalyst bed to measure the catalyst temperature. The oven temperature was controlled by a Eurotherm temperature controller. The catalysts were reduced *in situ* with 5% H₂ in N₂ for 1 h at 1125 K. After reduction, the temperature was lowered in Ar to the (initial) reaction temperature and the feed gas mixture (25% CH₄ (vol), 25% CO₂, 5% N₂, and 45% Ar for a total flow of 170 ml · min⁻¹) was switched to the reactor. The reaction products were analysed in a gas chromatograph (Varian 3300), equipped with two 3-m carbosieve columns and a TCD.

Pulse experiments. Pulse experiments were performed in an Altamira AMI-2000 apparatus. The Pt/ZrO₂ catalyst (500 mg) was reduced at 1125 K in a flow of 30 ml · min⁻¹ 5% H₂/N₂. Subsequently, the temperature was lowered to 925 K in He to remove any adsorbed hydrogen. The sample was continuously exposed to a flow of 30 ml · min⁻¹ He. The desired gas was pulsed into this He stream (pulse size 2.1 × 10⁻⁵ mol). The reaction products were quantified with a mass spectrometer. Conversions during the pulse

experiments were calculated as follows:

((area of the peak during pulsing over the catalyst)

– (area of the peak during pulsing over the catalyst))

* calibration factor.

Coke (CH_x) determination. The same setup as described above for the pulse experiments was used for the determination of the amount of carbonaceous deposits on used catalysts. The used catalyst (usually 150 mg) was heated to 1125 K in He to remove adsorbed water and CO₂. Subsequently O₂ was pulsed and the CO (m/e = 28) and CO₂ (m/e = 44) signals were measured with the mass spectrometer and quantified.

RESULTS

Catalytic Activity of Pt/ZrO₂ and Different Rh-Based Catalysts

In Fig. 1 the stability of Pt/ZrO₂ is compared with that of different Rh catalysts. The physico-chemical properties of these catalysts are summarized in Table 1. It can be seen from Fig. 1 that the stabilities of Rh/γ-Al₂O₃, Rh/ZrO₂, and Pt/ZrO₂ are comparable. The Rh-based catalysts are slightly more active than Pt/ZrO₂ (see Table 2). In contrast to Pt/SiO₂, Rh/SiO₂ has initially a good activity. However, this catalyst deactivated quickly and lost about 70% of its initial activity during 25 h time on-stream. After this period the catalyst showed a stable, but low activity. The Rh dispersion of this catalyst decreased by 74% in 25 h which indicates that the activity of this catalyst is linear proportional to the availability of Rh. These results indicate that

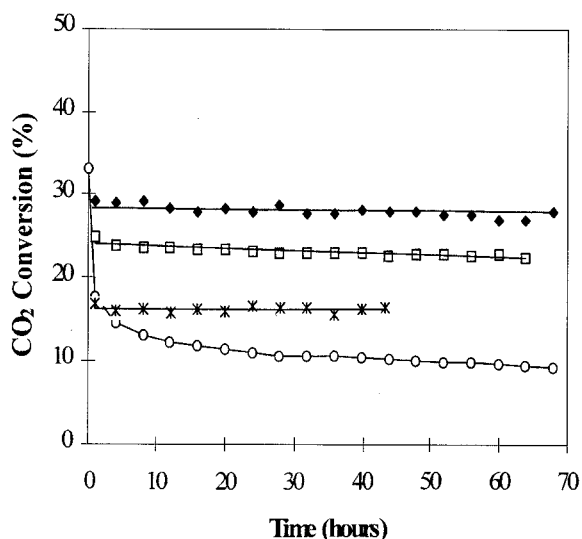


FIG. 1. Stability of Pt and Rh catalysts for CO₂/CH₄ reforming at 875 K, CO₂/CH₄/Ar/N₂ = 42/42/75/10 ml · min⁻¹: ◆ = Pt/ZrO₂ (300 mg), □ = Rh/γ-Al₂O₃ (50 mg), * = Rh/ZrO₂ (50 mg), ○ = Rh/SiO₂ (300 mg).

TABLE 1

Some Physico-Chemical Properties of the Catalysts

Catalyst	BET surface area (m ² /g)	Hydrogen chemisorption capacity (H/M)	Metal dispersion ^a (%)
Pt/ZrO ₂	17	1.1	100
Pt	—	0.001	0.1
Rh/ZrO ₂	18	1.5	90
Rh/γ-Al ₂ O ₃	110	0.46	68
Rh/SiO ₂	216	0.58	48
Rh	—	0.008	0.08

^aDispersions are calculated on basis of the hydrogen chemisorption capacity using the stoichiometries described by Kip *et al.* (34).

the activity of Rh catalysts is less influenced by the support since all Rh catalysts were active, whereas Pt catalysts which could not form carbonates on the support were two orders of magnitude less active compared to those that could (31). We have also shown (31) that the activity of the latter catalysts was determined by the concentration of Pt on the Pt–ZrO₂ perimeter. The lower importance of the support for Rh catalysts compared to Pt catalysts is also supported by the fact that the activity of Rh metal is much higher than that of Pt metal (see Table 3, note that the conditions used in this table are different from those used for the catalysts shown in Fig. 1). Because on Pt catalysts a special ensemble of sites located on the perimeter seems to determine the catalytic activity for CO₂/CH₄ reforming (31), the reaction mechanism was investigated in detail over Pt/ZrO₂ to address the influence of the support on the activity.

Interaction of Methane with Pt/ZrO₂

The results of pulsing methane over a freshly reduced catalyst, bare ZrO₂ and in an empty reactor are shown in Fig. 2. When methane was pulsed over a freshly reduced catalyst H₂ and traces of CO were the only observed products in the gas phase. Over ZrO₂ only a very small fraction of methane was converted (<1%). In an empty reactor methane was not converted under the reaction conditions used. In Fig. 3 the product distribution as a function of the amount of methane pulsed on the catalyst is shown (pulse

TABLE 2

Activity of Different Pt and Rh Catalysts (Conditions Described in Fig. 1)

Catalyst	Amount (mg)	CO ₂ conversion (%)	TOF of CO ₂ (s ⁻¹)
Pt/ZrO ₂	300	29	1.2
Rh/ZrO ₂	50	17	2.2
Rh/γ-Al ₂ O ₃	50	25	4.6
Rh/SiO ₂	300	33	1.2

TABLE 3

Comparison of the Activities of Pt and Rh Metal at 975 K,
 $\text{CO}_2/\text{CH}_4/\text{Ar}/\text{N}_2 = 50/50/170/30 \text{ ml} \cdot \text{min}^{-1}$

Catalyst	Amount of catalyst used (mg)	Amount of accessible metal ($\mu\text{moles/g}$)	CO_2 conversion (%)	TOF of CO_2 (s^{-1})
Pt	1000	53	1.5	0.2
Rh	50	78	10	9.6

size 2.1×10^{-5} moles CH_4). It can be seen from this figure that the rate of methane decomposition decreased with increasing amount of pulsed methane. When methane is decomposed stoichiometrically, molar H_2 yields double the molar methane conversion ($\text{CH}_4 \rightarrow 2\text{H}_2 + \text{C}$). However, the H_2 yield observed was only 1.2 times the methane converted indicating that some hydrogen is retained on the catalyst. The CO yield is significantly lower than the amount of methane converted. Thus, carbon containing species must be left on the catalyst surface. After the methane pulses, CO_2 was pulsed over this coke-containing catalyst. The only product observed in this experiment was CO . In Fig. 4 the CO_2 conversion and CO yield are plotted as functions of the amount of coke on the catalyst. As the amount of coke on the catalyst increased the CO_2 conversion and, thus, the CO yield increased. During all CO_2 pulsing experiments six pulses of CO_2 (126 μmoles) were given to the sample. Subsequently O_2 was pulsed over the catalyst to remove the remaining coke.

Table 4 shows the influence of the pretreatment of the catalyst with CO_2 on the methane conversion. The first row of this table compiles the product distribution during methane pulsing over a freshly reduced catalyst, while the

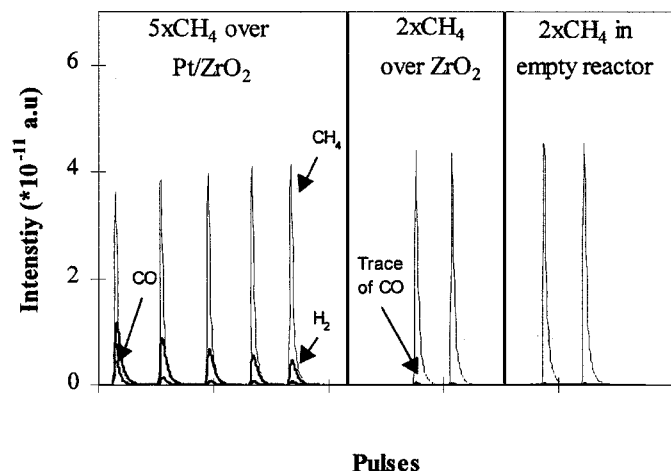


FIG. 2. Methane pulsing over Pt/ZrO_2 (left part of the figure), ZrO_2 (middle part of the figure), and in an empty reactor (right side of the figure) at 875 K (thin solid line: $m/e = 15$ (CH_4); higher thick solid line $m/e = 2$ (H_2); lower thick solid line: $m/e = 28$ (CO)).

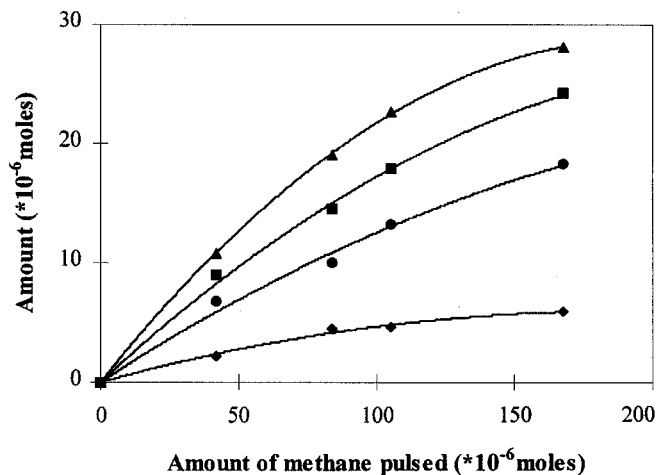


FIG. 3. Product distribution during methane pulsing over Pt/ZrO_2 at 875 K: \blacktriangle = H_2 yield, \blacksquare = CH_4 conversion, \bullet = CH_x (= carbon retained on the catalyst) yield, \blacklozenge = CO yield.

second row shows the results of methane pulsing over a catalyst pretreated with two pulses (42 moles) CO_2 . After exposing the catalyst to CO_2 the CH_4 conversion and the H_2 and CO yields increased. Both the $\text{H}_2\text{yield}/\text{CH}_4\text{converted}$ and $\text{COyield}/\text{CH}_4\text{converted}$ ratio did not significantly increase by pretreating the catalyst in CO_2 .

Interaction of Carbon Dioxide with Pt/ZrO_2

The transients observed during CO_2 pulsing over freshly reduced Pt/ZrO_2 are shown in Fig. 5. The results of pulsing CO_2 in an empty reactor tube and over the bare ("reduced") support are included in the same figure. It can be seen in Fig. 5 that CO_2 pulsing over freshly reduced Pt/ZrO_2 yields only CO ($\text{CO}_2 \rightarrow \text{CO} + \text{O}$) in the gas phase. When CO_2

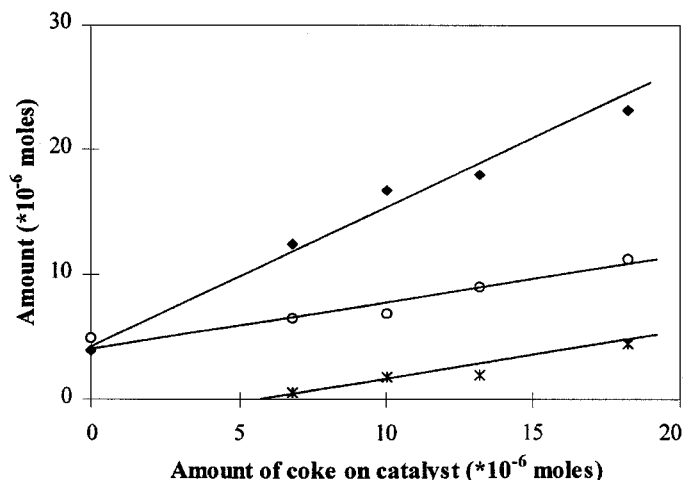


FIG. 4. Product distribution during CO_2 pulsing over coked Pt/ZrO_2 at 875 K: \circ = CO_2 conversion, \blacklozenge = CO yield, $*$ = CO_2 yield during subsequent O_2 pulsing.

TABLE 4
Influence of Pretreatment on Methane Conversion
over Pt/ZrO₂ at 875 K

Feed conditions		Conversion/yield (%)		
Pretreatment	Total amount of methane pulsed gas (μmol)	CH ₄	CO	H ₂
		H ₂	105	8.6
CO ₂ ^a	105	14.3	2.9	8.1

^a Two pulses (42 μmol) CO₂.

was pulsed over ZrO₂ or in an empty reactor, CO formation was not observed. Some CO₂ uptake (10%) was observed over ZrO₂. Possibly, CO₂ is adsorbed on ZrO₂ and is subsequently slowly desorbed, but it is not detectable in the background of the mass-spectrometer. The CO₂ conversions described in Fig. 4 are corrected for the "missing" 10% of CO₂ by adding 10% of the pulse size observed during CO₂ pulsing in an empty reactor to the observed pulse size.

The adsorption of CO₂ on Pt/ZrO₂ and ZrO₂ was also followed by time resolved i.r. spectroscopy at 775 K. The results of these experiments are shown in Figs. 6 and 7. When CO₂ was admitted to Pt/ZrO₂, i.r. bands were observed in two spectral regions. One band was characteristic for CO linearly adsorbed on Pt (2053 cm⁻¹). Its intensity decreased with prolonged exposure to CO₂ and after 10 min time on-stream it disappeared completely. Between 1300 and 1500 cm⁻¹ three broad bands were observed and tentatively attributed to surface carbonates (35). Similar bands were observed when pure ZrO₂ was contacted with CO₂ (see Fig. 7).

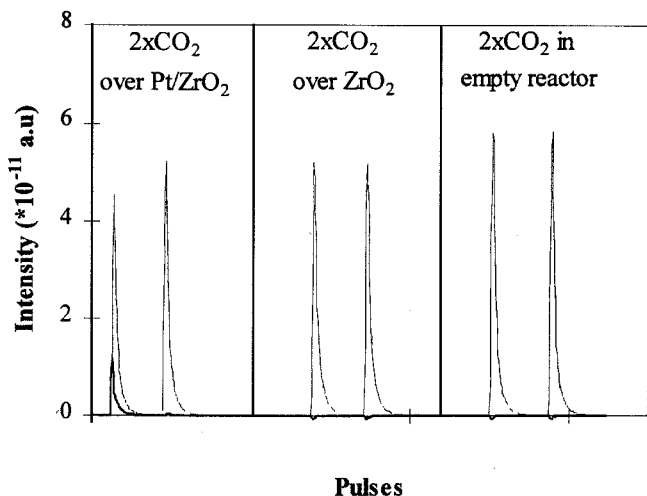


FIG. 5. Carbon dioxide pulsing over Pt/ZrO₂ at 875 K: thin solid line, $m/e = 44$ (CO₂); thick solid line, $m/e = 28$ (CO).

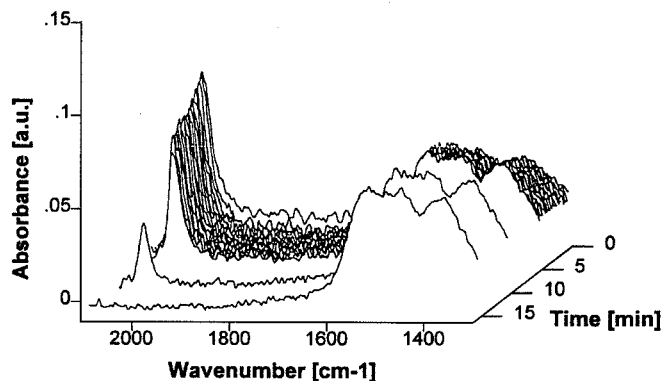


FIG. 6. Time resolved IR spectra during CO₂ adsorption on Pt/ZrO₂, $T = 775$ K, $p_{\text{CO}_2} = 0.25$, total flow 30 ml/min^{-1} .

While this indicates that CO₂ (at least initially) can dissociate CO₂ to CO and oxygen, the nature of the sorbed oxygen still needs to be addressed. Therefore, the catalysts were investigated by means of X-ray absorption spectroscopy in the presence of some of the reactants and products. Figure 8 shows the k^2 -weighted Fourier transformed EXAFS spectra of freshly reduced Pt/ZrO₂, and Pt/ZrO₂ which was exposed to CO₂ at 775 K for 20 min. For comparison, the spectra of the references, Pt and PtO, are also included. The radial distribution function of Pt/ZrO₂ did not show a peak at 1.8 Å after reduction indicating the absence of Pt–O bonds. Thus, we concluded that Pt is fully reduced. When the catalysts were subsequently exposed to CO₂ changes in the radial distribution function were not observed indicating that Pt did not oxidize. Figure 9 compiles the L_{III}-XANES of Pt/ZrO₂ in different atmospheres. The intensity of the white line of Pt in H₂ is similar to that of Pt in CO₂ while it was significantly more intense in oxygen.

DISCUSSION

Figure 1 demonstrates that Pt/ZrO₂ is an active and stable catalyst for CO₂/CH₄ reforming. We have shown

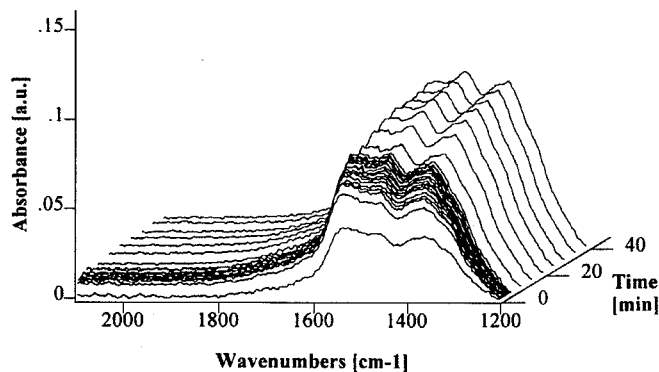


FIG. 7. Time resolved IR spectra during CO₂ adsorption on ZrO₂, $T = 775$ K, $p_{\text{CO}_2} = 0.25$, total flow 30 ml/min^{-1} .

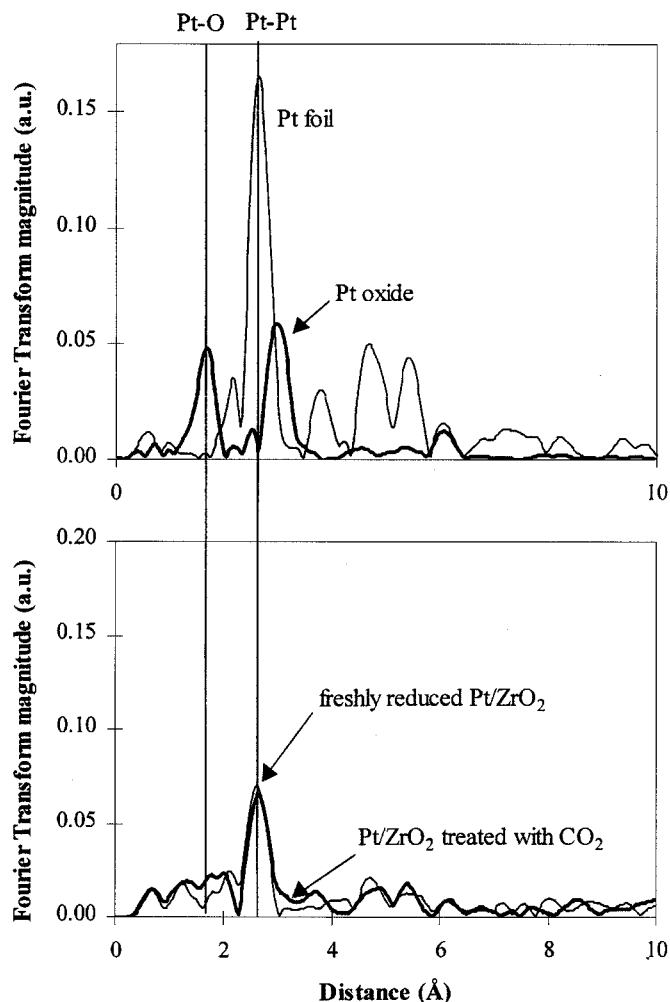


FIG. 8. k^2 -weighted Fourier transformed EXAFS spectra of Pt/ZrO₂ in the lower graph: fresh (thin line) and after 20 min CO₂ adsorption at 775 K (thick line). The references are plotted in the upper graph: Pt foil (thin line) and Pt oxide (thick line).

previously that the length of the Pt-ZrO₂ perimeter determines the activity of these catalysts (31). In line with previous suggestions by Nakamura *et al.* (29) and Zhang *et al.* (30) this suggests that the support/metal interface is important for the activity of the catalyst.

When methane was pulsed over freshly reduced Pt/ZrO₂, hydrogen and CO were observed as products (Fig. 2). By increasing the integral amount of methane pulsed to the sample, the methane conversion per pulse decreased (Fig. 3). This was attributed to a coverage of the metallic sites by coke. Increasing the carbon content on the catalyst decreased the rate of methane conversion. The importance of the support for CO formation over Pt/ZrO₂ and Pt/ γ -Al₂O₃ is shown in Table 5. Although both samples had the same pretreatment history, more CO was formed over Pt/ZrO₂ compared to Pt/ γ -Al₂O₃. This indicates that the ability of the support to release oxygen might be important

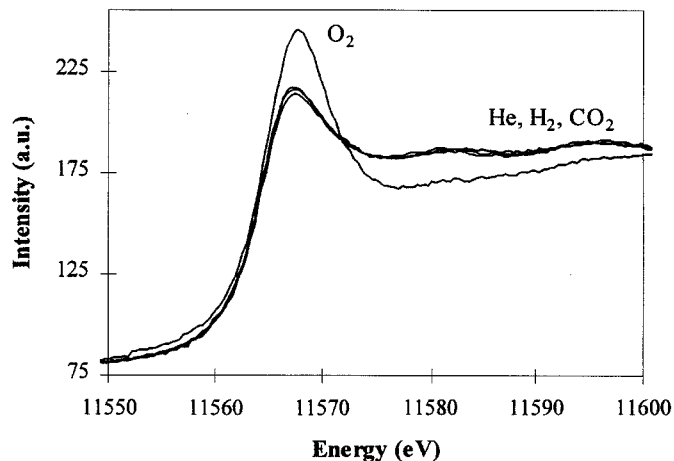


FIG. 9. XANES spectra of Pt/ZrO₂ in different atmospheres at 775 K.

to form CO. Indeed, different authors observed that ZrO₂ is, at least partially, reducible (36–40), whereas γ -Al₂O₃ is considered to be irreducible (41). One might speculate that the hydrogen treatment partially reduced the support but that the concomitantly formed water remains adsorbed on the catalyst surface. These OH groups might react with methane to yield CO and hydrogen. Table 5 also shows that Pt/ γ -Al₂O₃ is more active in methane decomposition compared to Pt/ZrO₂. However, note that such higher rates of coke formation (during methane pulses) are not necessarily related to the faster deactivation of the catalyst, because deactivation also critically depends on the rate with which the coke can be removed by CO₂ under reaction conditions.

From the CO₂ pulse experiments described in Fig. 5 we conclude that Pt/ZrO₂ is able to dissociate CO₂ to CO and adsorbed oxygen (O₂ was not observed in the gas phase). When CO₂ was pulsed over ZrO₂ 10% of the pulse was consumed without forming CO (Fig. 5). I.r. experiments of CO₂ adsorption on Pt/ZrO₂ and ZrO₂ show that this can be attributed to the formation of carbonates on the support (Fig. 7) (35). This also explains the CO₂ uptake observed during CO₂ pulsing over ZrO₂. The CO₂ is adsorbed on the support as a carbonate which is subsequently slowly released to the gas phase or is available for chemical reactions.

In summary, Pt/ZrO₂ is able to dissociate carbon dioxide to adsorbed CO and oxygen, and methane to adsorbed CH_x

TABLE 5
Comparison of Methane Dissociation Activity of Pt/ZrO₂ and Pt/ γ -Al₂O₃ at 875 K

Catalyst	Feed conditions Total amount of pulsed gas (μ mol)	Conversion/yield (%)		
		CH ₄	CO	H ₂
Pt/ZrO ₂	42	21.4	4.8	13.1
Pt/ γ -Al ₂ O ₃	42	30.9	2.4	23.8

and H₂. As CH₄ did not decompose on ZrO₂, it is concluded that methane dissociation occurs exclusively on Pt. Also for CO₂ dissociation Pt seems to be indispensable. However, it appears that the CO₂ dissociation is facilitated when a proper support is available, because a catalyst which did not form carbonates (Pt/SiO₂) did not show the formation of CO when exposed to CO₂. This leads to the conclusion that CO was not formed directly from CO₂ but from a (metal mediated) decomposition of the carbonate.

The adsorbed coke from decomposed methane can be removed by pulsing carbon dioxide (see Fig. 4). Twice the amount of CO was formed compared to the amount of CO₂ pulsed. This indicates that coke was removed by CO₂ (CO₂ + CH_x ⇌ 2CO + x/2H₂). Note that the removal of carbon with CO₂ was observed by Mark *et al.* for Rh/Al₂O₃ (17, 23). Above a coke concentration of 7 * 10⁻⁶ moles/500 mg catalyst (see Fig. 4) not all coke was removed by CO₂, because subsequent oxygen pulsing revealed the formation of CO₂. Thus, we speculate that methane pulsing leads to the formation of two types of coke deposited. One type can be removed with CO₂, the other type only with oxygen.

Although coke formed could be removed by CO₂ and O₂, hydrogen which was still present at the surface is apparently not removed (as discussed above the H_{2,yield}/CH_{4,converted} = 1.2 (during methane pulsing), whereas a ratio of 2 was expected). As neither hydrogen nor water were observed during the CO₂ pulses, we conclude that the hydrogen is retained on the catalyst surface. We think that the adsorbed hydrogen reacts with adsorbed oxygen from CO₂ dissociation to form surface OH groups. Because water was not observed as a product during the methane pulse experiments, we conclude that it remains on the catalyst surface. The hydrogen balance under steady state conditions is always 100%. Thus, the formation of OH groups on the catalyst is a transient effect during the pulse experiments. Under steady state conditions, i.e. once all sites are saturated, the OH groups might desorb as water or react further with methane to form hydrogen and CO (steam reforming).

From Fig. 4 it is seen that preexposure of the catalyst to methane (coke formation) enhanced the CO₂ conversion and CO yield. On the other hand, preexposure of the catalyst to CO₂ followed by methane pulsing showed an enhanced methane conversion, compared to methane pulsing over a freshly reduced catalyst (Table 1). This indicates that the presence of mutually generated carbon/oxygen species enhance the activation of the other components (see also suggestions by Solymosi *et al.* and Erdöhelyi *et al.* (12, 24)).

I.r. spectroscopy demonstrates that CO₂ can be dissociated to CO and adsorbed oxygen (Fig. 6). The decrease of the concentration of sorbed CO with time on stream is explained by blocking of the sites that decompose CO₂ with the oxygen that is concomitantly formed (self-poisoning). However, the EXAFS experiments did not give evidence

for the presence of adsorbed oxygen or (surface) oxides of Pt-O so it is not likely that the oxygen is located on Pt. This is also supported by the XANES experiments as the intensity of the white line did not increase in the presence of CO₂ (Fig. 9). Such an increase is expected when Pt is oxidized (42) or when strongly electronegative groups are adsorbed. Thus, we conclude that the oxygen is consumed by the support at the metal-support interface. This oxygen can be released again in the form of CO when methane is pulsed over the catalyst, as was described above. Therefore, we would like to speculate that the formation of CO is limited to the presence of oxygen defects of the support at the interface. Once these are filled the formation of CO stops. Note that this will lead to the disappearance of sorbed CO as at the reaction temperature sorbed CO has only been observed in the presence of gas phase CO.

In addition to CO formation, the i.r. spectra revealed the formation of carbonate species (35, 43) on ZrO₂. Pt-based catalysts which did not show the formation of carbonates, such as Pt/SiO₂ and Pt-black, had a very low reforming activity. This clearly indicates that for Pt-based catalysts the ability to form carbonates is important for the activity of the catalyst. In order to form CO from CO₂ at least one of the C-O bonds must be broken. Note that for reactions in which C-O bond breaking was involved (CO/CO₂ methanation) it was shown that the presence of a support enhanced the activity of the catalysts compared to unsupported catalysts (14, 30, 44-48). This was explained by a weakening of the C-O bond when CO/CO₂ was adsorbed with the carbon on the support and the O-atom on the metal, i.e., at the metal-support perimeter. This was claimed to facilitate the dissociation of the C-O bond and is in perfect agreement with our observation.

In summary, methane can be decomposed on Pt. The carbon left from this reaction can be removed CO₂. CO₂ adsorbs on the support and forms carbonates. When carbonates were formed the activity of the catalyst was high. Additionally, the activity of Pt/ZrO₂ has been shown to be linearly proportional to the concentration of the Pt-ZrO₂ perimeter. Based on these observations we propose a mechanism which involves the activation of methane on Pt and activation of CO₂ on the support. At the Pt-ZrO₂ perimeter the activated species combine to form two CO molecules (Fig. 10). The figure shows the different possibilities of CO₂

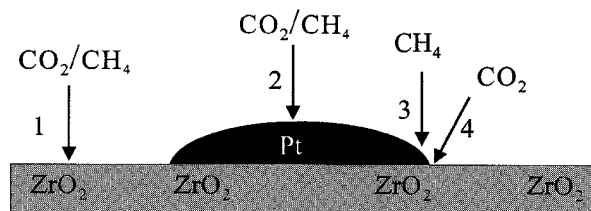


FIG. 10. Possible adsorption sites for CO₂ and CH₄ on Pt/ZrO₂.

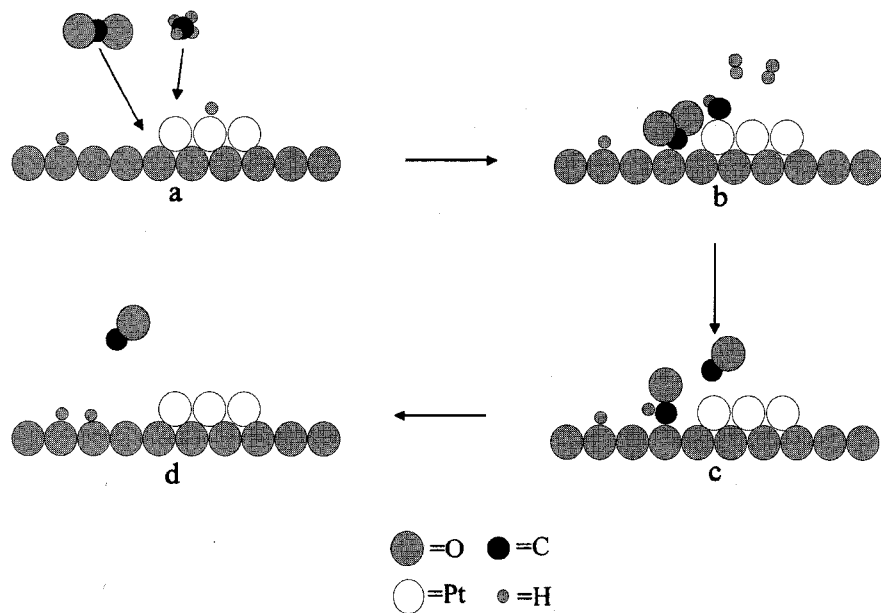


FIG. 11. Schematic representation of the proposed mechanism of CO_2/CH_4 reforming over Pt-ZrO_2 : (a) CO_2 adsorbs on the support as carbonate, methane decomposes on the metal. (b) + (c) The coke species on the metal reduces the carbonate to a formate while CO is formed. (c) The formate decomposes to OH and CO . Note that under steady state conditions OH groups and adsorbed hydrogen are presumed to be present.

and CH_4 to adsorb on Pt/ZrO_2 . *Pathway 1* leads to the formation of carbonate species and coke on the support. *Pathway 2* leads to the formation of hydrogen and CO directly on the Pt. This pathway can be neglected on Pt catalysts because Pt-black has a low catalytic activity. However, on Rh catalysts this route contributes significantly to the overall activity of the catalysts, because Rh metal has an appreciable activity for reforming (about 50 times more active at 925 K). This was concluded by work from Mark *et al.* who showed that CO_2/CH_4 reforming occurs via an Eley-Rideal type mechanism on $\text{Rh}/\gamma\text{-Al}_2\text{O}_3$ (17, 23). In *Pathways 3 and 4* methane is dissociated on the Pt particle in the vicinity of the Pt-ZrO_2 perimeter, generating CH_x type species on Pt and H_2 in the gas phase. Carbon dioxide is activated on the support in the vicinity of the Pt particle to form a carbonate. The carbonate might be reduced by the CH_x species to form formate and CO . The formate decomposes rapidly (48) to CO and an adsorbed OH group. The OH groups can either recombine and desorb as water or react further with CH_x to form CO and hydrogen (steam reforming). Note that also the reverse water gas shift reaction occurs on these catalysts, thus, an equilibrium between hydrogen and water (OH groups) exists. The mechanism of CO_2/CH_4 reforming is schematically shown in Fig. 11.

CONCLUSIONS

The activity of Rh catalysts for CO_2/CH_4 reforming is mainly determined by the availability of Rh irrespective of the support. For Pt catalysts the support plays an important

role in the activity. The CO_2 and CH_4 react via two different sites over Pt/ZrO_2 (bifunctional mechanism). Pulse experiments show that methane is decomposed on the metal (Pt) to form CH_x and hydrogen. I.r. spectroscopy of CO_2 adsorption on the catalyst revealed the formation of carbonates on the support and of CO , during a transient period, adsorbed on Pt. Catalysts which were incapable of forming carbonates were almost inactive for reforming. The activity of Pt/ZrO_2 depended linearly on the Pt-ZrO_2 perimeter concentration. On basis of these results a mechanism is proposed in which the carbonate on the Pt-ZrO_2 perimeter is reduced by the CH_x species on the metal to form CO and a formate species. Subsequently, the formate is decomposed to CO and an OH group which remains on the surface. Under steady state conditions, the OH groups might either desorb as water or react with methane to form CO and hydrogen (steam reforming).

ACKNOWLEDGMENTS

This project was supported by the EU, Joule II programme, sub-programme: Energy from fossil sources: hydrocarbons, Contract J0U2-CT92-0073. The XAS measurements were carried out at the SRS, Daresbury Laboratory, United Kingdom, Grant 27/251. The authors are indebted to M. Englisch and A. Jentys for valuable discussions on XAS of Pt/ZrO_2 .

REFERENCES

1. Ashcroft, A. T., Cheetham, A. K., Green, M. L. H., and Vernon, P. D. F., *Nature* **225**, 352 (1991).
2. Richardson, J. T., and Paripatyadar, S. A., *Appl. Catal.* **61**, 293 (1990).

3. Seshan, K., and Lercher, J. A., "Carbon Dioxide: Environmental Issues" (J. Paul and C. Pradier, Eds.), p. 16. Royal Soc. Chem., Cambridge, 1990.
4. Bhattacharya, A., and Chang, V. W., *Stud. Surf. Sci. Catal.* **88**, 207 (1994).
5. Kurz, G., and Teuner, S., *Erdol. Kohle* **43**(5), 171 (1990).
6. van den Oosterkamp, P. F., Chen, Q., Overwater, J. A. S., Ross, J. R. H., and van Keulen, A. N. J., in "Meeting of Large Chemical Plants, Antwerp, Belgium, Oct. 1995."
7. Udengaard, N. R., Bak Hansen, J. H., Hanson, D. C., and Stal, J. A., *Oil Gas J.* **90**, 62 (1992).
8. Qin, D., and Lapszewicz, J., *Catal. Today* **21**, 551 (1994).
9. Perera, J. S., Sankar, J. W., and Thomas, J. M., *Catal. Lett.* **11**, 219 (1991).
10. Teuner, S., *Hydrocarbon Processing*, 106 (May 1985).
11. Fischer, F., and Tropsch, H., *Brennst. Chem.* **39** (1928).
12. Solymosi, F., Kutsan, Gy., and Erdöhelyi, A., *Catal. Lett.* **11**, 149 (1991).
13. Vernon, P. D. F., Green, M. L. H., Cheetham, A. K., and Ascroft, A. T., *Catal. Today* **13**, 417 (1992).
14. Nakamura, J., Aikawa, K., Sato, K., and Uchijima, T., *Catal. Lett.* **25**, 265 (1994).
15. Rostrup Nielsen, J. R., and Bak Hansen, J. H., *J. Catal.* **144**, 38 (1993).
16. Tsipouriari, V. A., Efstathiou, A. M., Zhang, Z. L., and Verykios, X. E., *Catal. Today* **21**, 579 (1994).
17. Mark, M. F., and Maier, W. F., *Angew. Chim. Int. Ed. Engl.* **33**(15/16), 1657 (1994).
18. Sakai, Y., Saito, H., Sodesawa, T., and Nozaki, F., *React. Kinet. Catal. Lett.* **24**, 253 (1984).
19. Seshan, K., ten Barge, H. W., Hally, W., van Keulen, A. N. J., and Ross, J. R. H., *Stud. Surf. Sci. Catal.* **81**, 285 (1994).
20. Bitter, J. H., Hally, W., Seshan, K., van Ommen, J. G., and Lercher, J. A., *Catal. Today* **29**, 349 (1996).
21. Lercher, J. A., Bitter, J. H., Hally, W., Niessen, W., and Seshan, K., *Stud. Surf. Sci. Catal.* **101**, 463 (1996).
22. Seshan, K., Mercera, P. D. L., Xue, E., and Ross, J. R. H., *German Patent P4313673* (1994), *International Patent WO94/224042* (1994).
23. Mark, M. F., and Maier, W. F., *J. Catal.* **164**, 122 (1996).
24. Erdöhelyi, A., Cerenyi, J., and Solymosi, F., *J. Catal.* **141**, 287 (1993).
25. Bradford, M. C. J., and Vannice, M. A., *Appl. Catal. A: General* **142**, 97 (1996).
26. Qin, D., Lapszewicz, J., and Jiang, X., *J. Catal.* **159**, 140 (1996).
27. Bodrov, I. M., and Apel'baum, L. O., *Kinet. Katal.* **8**, 379 (1967).
28. Bodrov, I. M., Apel'baum, L. O., and Temkin, M. I., *Kinet. Katal.* **8**, 821 (1967).
29. Nakamura, J., Aikawa, K., Sato, K., and Uchijima, T., *Catal. Lett.* **25**, 265 (1994).
30. Zhang, Z., Verykios, X. E., MacDonald, S. M., and Affrossman, S., *J. Phys. Chem.* **100**, 744 (1996).
31. Bitter, J. H., Seshan, K., and Lercher, J. A., *J. Catal.* **171**, 279 (1997).
32. Paal, Z., Zhan, Z., Fulop, E., and Tesche, B., *J. Catal.* **156**, 19 (1995).
33. "Vogel's Quantitative Inorganic Analysis," 3rd ed., p. 474, revised by J. Bassett, R. C. Denney, G. H. Jeffery, and J. Mendham, Chaucer Press, 1978.
34. Kip, B. J., Duivenvoorden, F. B. M., Koningsberger, D. C., and Prins, R., *J. Catal.* **105**, 26 (1987).
35. Bensitel, M., Saur, O., and Lavalley, J. C., *Mater. Chem. Phys.* **17**, 249 (1987).
36. Trunschke, A., Hoang, D. L., and Lieske, H., *J. Chem. Soc. Faraday Trans.* **91**(24), 4441 (1995).
37. Morterra, C., Giamell, E., Oria, L., and Volante, M., *J. Phys. Chem.* **94**, 311 (1990).
38. Hoang, D.-L., and Lieske, H., *Catal. Lett.* **27**, 33 (1994).
39. Tulier, P., and Martin, G. A., *React. Kinet. Catal. Lett.* **21**, 287 (1982).
40. Dall'Agnol, C., Gervasini, A., Morazonni, F., Pinna, F., Stukol, G., and Zanderighi, L., *J. Catal.* **96**, 106 (1985).
41. Rynkowsky, J. M., Paryjczak, T., Lenik, M., Farbotko, M., and Goralski, J., *J. Chem. Soc. Faraday Trans.* **91**, 3481 (1995).
42. Englisch, M., Lercher, J. A., and Haller, G. L., "X-Ray Absorption Fine Structure for Catalysts and Surfaces" (Y. Iwasawa, Ed.), p. 275. World Scientific, Singapore, 1996.
43. Little, L. H., "Infrared Spectra of Adsorbed Species," p. 77. Academic Press, London, 1966.
44. Boffa, A. B., Bell, A. T., and Somorjai, A., *J. Catal.* **139**, 602 (1993).
45. Sachtler, W. M. H., Shriver, D. F., Hollenber, W. B., and Lang, A. F., *J. Catal.* **92**, 429 (1985).
46. Demmin, R. A., and Gorte, R. J., *J. Catal.* **98**, 577 (1986).
47. Fukuoka, A., Kimura, T., Rao, L.-F., and Ichikawa, M., *Catal. Today* **6**, 55 (1989).
48. Rhodes, C., Hutchings, G. J., and Ward, A. M., *Catal. Today* **23**, 43 (1995).